New Approach to High-Fidelity Aerodynamic Design Optimization of a Wind Turbine Blade

M.H. Djavareshkian *‡, A. Latifi Bidarouni *, M.R.Saber *

*Department of Mech. Engg., Faculty of Engg., Ferdowsi University of Mashhad, Mashhad, Iran

(javareshkian@um.ac.ir ,a.latifi.b@gmail.com, mrs_mechanic@yahoo.com)

‡ Corresponding Author; Mechanical Engineering Department., Faculty of Engineering., Ferdowsi University of Mashhad, Mashhad, Iran M.H. Djavareshkian, Tel: +98 511 880 5037, javareshkian@um.ac.ir

Received: 14.08.2013 Accepted:13.09.2013

Abstract-A new approach to high-fidelity aerodynamic design optimization of a wind turbine blade configuration is offered. This method combines Blade Element Momentum (BEM) theory with the high fidelity aerodynamic shape optimization of an airfoil. The chord length and the twist angle of the blade at various radiuses have been calculated by BEM. The Navier Stokes equations are solved to simulate both two and three dimensional flows. The Results which are obtained from 2D Computational Fluid Dynamics (CFD) have been utilized to train a Neural Network (NN). E387 Eppler is used as the base cross section of the blade. In the process of airfoil optimization, Genetic Algorithm (GA) is coupled with trained NNto attain the best airfoil shape at each angle of the attack. The simulation and validation of the base wind turbine with calculated pitch angle, twist angle, chord profile and base airfoil have been performed. The comparison of the results of this turbine with optimized one, illustrates a significant improvement in power factor.

Keywords Wind turbine blade, NN, GA, NVD, BEM.

1. Introduction

In recent years, wind has become an increasingly attractive source of renewable energy. Wind energy is the world's fastest-growing energy technology. The optimization of wind turbines has an important role to capture as much energy as possible from the wind. Designing new airfoils are essential to produce a wind turbine with higher efficiency. This has been studied by several authors [1-5]. Optimizations with High fidelity models are expensive even for two dimensional cases. Therefore surrogate models are applied in some researches [3, 6-8]. The flow around a wind turbine is three dimensional, therefore, distinguishing the other important parameters like chord, twist and pitch angle profiles as well as complete blade configuration were the subject of many other studies[9-14]. BEM method is capable to calculate the steady loads and thus also the thrust and power for different settings of wind speed, rotational speed and pitch angle[15]. It's also a quick and simple method, therefore application of BEM is prevalent in wind turbine studies [16-18]. BEM theory usually is uses for evaluating the forces on the wind turbine in its design and optimization.

In this paper, a new approach to high-fidelity aerodynamically optimization of a wind turbine blade is presented. Twist and chord profile have been determined by BEM. The absolute angle of attack of the blade at each cross section is different because of differences in twist angle and tangential velocity component related to angular velocity. In this article, high-fidelity optimization is applied to determine the appropriate airfoil shape at various cross sections. High-fidelity simulation is also applied to calculate the aerodynamic characteristics of the wind turbine. Employing a surrogate model like neural network is critical to make this idea practical, because not only NN reduces the cost of optimization substantially but also speed it up. The results confirm that this method yield considerable increase in power factor.

2. Methodology

2.1. Governing equation and discretization

The basic equations which describe the conservation of mass, momentum and scalar quantities can be expressed in

the following vector forms which are independent in the

$$\frac{\delta\rho}{\delta t} + div\left(\rho\vec{V}\right) = S_m \quad \textbf{(1)}$$

$$\frac{\delta(\rho\vec{V})}{\delta t} + div\left(\rho\vec{V}\otimes\vec{V} - \vec{T}\right) = \vec{S}_v \quad \textbf{(2)}$$

$$\frac{\delta(\rho\phi)}{\delta t} + div\left(\rho\vec{V}\phi - \vec{q}\right) = \vec{S}_\phi \quad \textbf{(3)}$$

coordinate system.

The last two equations are usually expressed in terms of basic dependent variables. The stress tensor for a Newtonian

$$\vec{T} = -P\vec{I} \quad \textbf{(4)}$$

fluid is:

and the Fourier-type law usually gives the scalar flux

$$\vec{q} = \Gamma_\phi grad\phi \quad \textbf{(5)}$$

vector:

In this study, $k-\varepsilon$ model is utilized for turbulence flow. The $k-\varepsilon$ model is simple and has good stability with easy convergence. The discretization of the above differential equations is carried out by using a finite-volume approach. First, the solution domain is divided into a finite number of discrete volumes or cells, where all variables are stored at their geometric centers (see e.g. Fig.1).

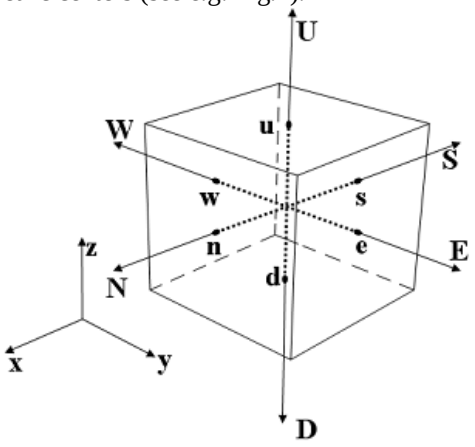

Fig.1. Finite volume and storage arrangement

The equations are then integrated over all the control volumes by utilizing the Gaussian theorem. The discrete expressions are presented to refer to only one face of the control volume, namely, e, for the sake of brevity. For any variable ϕ (which may also stand for the velocity components), the result of the integration yields:

$$\frac{\delta v}{\delta t}\left[\left(\rho\phi\right)_p^{n+1} - \left(\rho\phi\right)_p^{n}\right] + I_e - I_w + I_n - I_s + I_u - I_d = S_\phi \delta v \quad \textbf{(6)}$$

Where $I's$ are the combined cell-face convection I^c and diffusion I^D fluxes. The diffusion flux is approximated by central differences. The discretization of the convective flux requires special attention and it causes to develop the various schemes. A representation of the convective flux for

$$I_e^c = \left(\rho.V.A\right)_e \phi_e = F_e\phi_e \quad \textbf{(7)}$$

cell-face (e) is:

The value of ϕ_e is not known and it should be estimated from the values at neighboring grid points by interpolation. The expression for the ϕ_e is determined by the SBIC scheme [19], that is based on the NVD technique [20] using interpolation from the nodes E, P and W. The functional relationship utilized in SBIC scheme for $\bar{\phi}_e$ is presented as:

$$\bar{\phi}_e = \bar{\phi}_p, \qquad IF\ \bar{\phi}_p \notin [0,1]$$

$$\bar{\phi}_e = \frac{\bar{x}_p - \bar{x}_e}{K\left(\bar{x}_p - 1\right)}\bar{\phi}_p^{\,2} + \left(1 + \frac{\bar{x}_p - \bar{x}_e}{K\left(\bar{x}_p - 1\right)}\right)\bar{\phi}_p, \quad IF\ \bar{\phi}_p \in [0,K] \quad \textbf{(8)}$$

$$\bar{\phi}_e = \frac{\bar{x}_p - \bar{x}_e}{\bar{x}_p - 1} + \frac{\bar{x}_p - \bar{x}_e}{\bar{x}_p - 1}\bar{\phi}_p, \qquad IF\ \bar{\phi}_p \in [K,1]$$

Where

$$\bar{\phi}_p = \frac{\phi_p - \phi_W}{\phi_E - \phi_W}, \qquad \bar{\phi}_e = \frac{\phi_e - \phi_W}{\phi_E - \phi_W}$$

$$\bar{x}_p = \frac{x_p - x_W}{x_E - x_W}, \qquad \bar{x}_e = \frac{x_e - x_W}{x_E - x_W} \quad \textbf{(9)}$$

The limits on the selection of K could be determined by the following ways. Obviously, the lower limit is $K = 0$ which would represent switching between upwind and central difference. It is not favorable, because it is essential to avoid the abrupt switching between the schemes in order to achieve the converged solution. The value of K should be kept as low as possible in order to attain the maximum resolution of the scheme. The final form of the discretized

$$a_p.\phi_p = \sum_{m=E,W,N,S} a_m.\phi_m + S_\phi^{'} + S_{dc} \quad \textbf{(10)}$$

equation from each approximation is given as:

Where, $a's$ are the convection-diffusion coefficients. The term $S_{\phi}^{'}$ in Eq. 10 contains quantities arising from non-orthogonality, numerical dissipation terms and external sources. For the momentum equations, it is easy to separate out the pressure-gradient source from the convection momentum fluxes. S_{dc} is the contribution due to the adapted deferred correction procedure.

2.2. Hicks-Henne function

To produce a smoothed shape airfoil with a few numbers of design variables, Hicks-Henne functions have been utilized in this work. The geometry of new airfoil can be

$$y_{new} = y_{base} + \sum_{i=1}^{n} \alpha_i f_i \qquad \textbf{(11)}$$

obtained with Eq. 11 [21].

Where y_{new} is the y coordinate of new airfoil, y_{base} is the y coordinate of base airfoil which in this research, Eppler E387 airfoil coordinate has been selected. α_i, $(i = 1, 2, .., 16)$ are design variables. Eight design variables have been considered for upper side of airfoil $(\alpha_1 \, to \, \alpha_8)$ and other eight design variables have been looked upon for lower side of airfoil $(\alpha_9 \, to \, \alpha_{16})$. This means that there are sixteen design variables totally which will be generated by GA at each generation. $f_i \; (\; i = 1, 2, .., 8)$ are shape

$$f_k(x) = \sin\left(\pi (1-x)^{e(k)}\right), \qquad \textbf{k=1,2} \qquad \textbf{(12)}$$

$$f_k(x) = \sin^3\left(\pi x^{e(k)}\right), \qquad \textbf{k=3,4,5} \qquad \textbf{(13)}$$

$$f_k(x) = \sin\left(\pi x^{e(k)}\right), \qquad \textbf{k=6,7,8} \qquad \textbf{(14)}$$

functions and should be calculated from Eqs. 12 to14.

Where x is the coordinate of airfoil related to y_{base} or y_{new} , k is the number of design variables on each side of

$$e(k) = \ln 0.5 / \ln(1 - x_k) \qquad \textbf{k=1,2} \qquad \textbf{(15)}$$

$$e(k) = \ln 0.5 / \ln(x_k) \qquad \textbf{k=3,4,5,6,7,8} \qquad (16)$$

airfoil and $e(k)$ can be calculated from Eqs. 15 and 16.

Where x_k, $(k = 1, 2, \ldots, 8)$ determines where maximum of f_k occurs and is sundry from x. values for x_k which have been applied in this work are illustrated in Table 1.

Table 1. The values of x_k which have been used

x_1	x_2	x_3	x_4	x_5	x_6	x_7	x_8
0.08	**0.15**	**0.20**	**0.30**	**0.45**	**0.60**	**0.75**	**0.92**

It's prominent to note that each of design variables must be bounded to a certain range, because GA can just search in a region that has been assigned to it. The wider region increases the chance of finding a better solution, but it will take more time. Accordingly, the range which assigned to each design variable should be determined somehow to possess a good compromise between gaining a better solution and time. Shadowed area in Fig.2illustrates the domain where Genetic Algorithm searches to find the optimum solution.

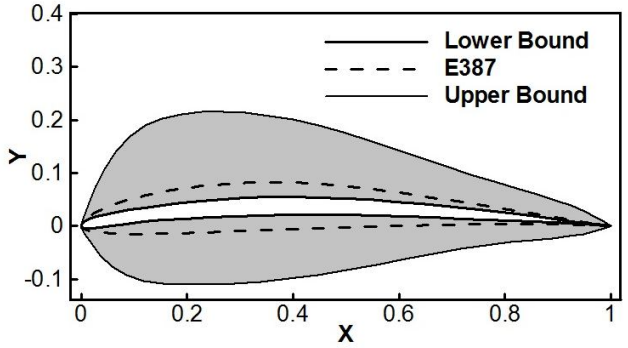

Fig.2. The illustration of domain where Genetic Algorithm searches

2.2. Boundary condition

For two dimensional cases, velocities are prescribed at the inlet of the domain and the pressure is obtained by zero order extrapolation from interior points. At outlet, the pressure is fixed. The far-field boundary is set to 30c from the airfoil to minimize its undesired effects on the flow surrounding and is set to slip boundary conditions. The non-slip condition is applied at the airfoil surfaces. To account for the steep variations in turbulent boundary layers near solid walls, wall functions which define the velocity profile in the vicinity of no-slip boundaries are employed. For three dimensional cases, the boundary condition for inlet, outlet and blade are set to velocity inlet, pressure outlet and wall respectively. Moreover, the slip boundary is used for other boundaries. The domain and boundary conditions of the wind turbine are illustrated in Fig.3.

2.3. Optimization algorithm and objective function

Optimization method which is applied in this research is Genetic Algorithm (GA). GA is a stochastic optimization method to find the minimum or maximum of a problem as the best solution. The principles of genetics and natural selection which is introduced by Darwin as evolution theory is the basis of GA. Elaborate details about GA can be found in[22].

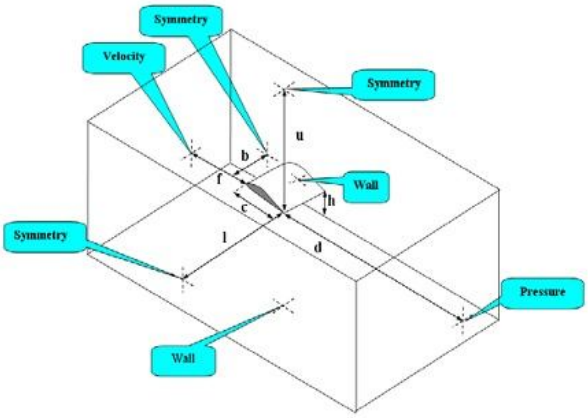

Fig.3 . The domain and boundary conditions of the wind turbine

Maximizing lift to drag ratio is considered as objective function for all optimizations which have been done in this research. The mathematics expression for objective function

Maximizing: L/D **at absolute AOA**

Subject to : **(17)**

$$lower\ bound < \alpha_i < uper\ bound$$

is expressed in Eq. (17) .

2.4. Neural Network (NN)

Neural Network (NN) is a simple model of biological neurons. Neural networks are good in fitting functions to any set of practical data. Network architecture that is used in this research is illustrated inFig.4.This is a feed forward network with 3 layers.

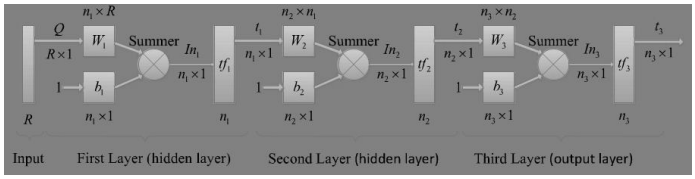

Fig.4. The architecture of Artificial network used[23]

Table 2 manifests a sample data as NN's input for one random airfoil. This is a small part of entire input data. It is notable that for any airfoil, all rows are the same and just seventeenth column which the angle of attack is changed.

The output of network can be calculatedfrom Eq. (18)

$$a_3 = tf_3\left(W_3 tf_2\left(W_2 tf_1\left(W_1 q + b_1\right) + b_2\right) + b_3\right) \quad \textbf{(18)}$$

[23].

Table 2. The sample of data as Neural Network's input

α_1	α_2	. .	α_{15}	α_{16}	*AOA*
0.027996	**0.00272**	. .	**0.007363**	**0.002982**	**0**
0.027996	**0.00272**	. .	**0.007363**	**0.002982**	**6**
. . .	. . .	. .	. . .	. . .	. . .
0.027996	**0.00272**	. .	**0.007363**	**0.002982**	**18**
0.027996	**0.00272**	. .	**0.007363**	**0.002982**	**20**

Number of neurons in first layer R is equal to the number of problem's input.The number of neurons for the output layer n_3 is equal to the number of problem's output. It is desirable that NNpredicts the values of lift, drag and moment coefficients about one fourth of chord from leading edge related to each set of Network's input.Therefore, here, the number of output is three. Table 4 shows sample data as NN's target and related to those data in Table 3.In an ideal trained neural network, the outputs of NN must be equal to the targets.

Table 3. The sample of data as NN's target and related to those data in Table 2

C_l	C_d	$C_{m_{c/4}}$
0.225871	**0.038546**	**-0.0422**
0.77316	**0.054639**	**-0.04163**
. . .	. . .	. . .
1.162999	**0.198523**	**-0.04913**
1.071324	**0.23491**	**-0.05597**

There is no certain method to determine the other parameters of network architecture. These parameters which are the number of layers and the number of neurons in each one must be determined by try and error. Here, several networks with various network architecture i.e. sundry numbers of layers and different numbers of neurons in each layer have been examined to define the appropriate network architecture. For all examined networks, transfer function of hidden layers is Hyperbolic Tangent Sigmoid and transfer function for output layer is linear. The Levenberg-Marquardt learning algorithm is applied, because the network is relatively small and this algorithm is fast and efficient for this kind of networks [24] and also it is proper for the purpose of function fitting [23]. The Mean Square Error

(MSE) is selected as NN's performance. Training algorithm adjust weights in a way to minimize the MSE.

2.5. Procedures

2.5.1. Blade Profile Design

The chord profile and twist angle of the blade have been determined at each cross section of the blade by BEM method.The absolute angles of attack at some radiuses are calculated because it varies locally alongside the blade.

2.5.2. Airfoil Optimization

The GA is coupled with CFD to create and analyze manyairfoils.The results of numerical simulation are utilized to train various NN architectures. When several NN architectures are examined, then the network architecture with lower MSE is elected as trained NN.The flow chart applied in this paper for NN training illustrated in Fig.5.

Then the trained NN has been appliedfor the rest optimization processes with any desirable objective function. Flow chart of optimization with GA coupled with trained NN demonstrated inFig.6.In the present research, the training process is separated from optimization procedure. Therefore,any optimization with any objective function can be performed with this trained NN. There is no need to do more CFD simulation for new optimizations.

2.5.3. Wind Turbine Simulation

Several simulation of wind turbine with different domain length and various grid sizes have been carried out to find the best dimensions. The validation of numerical results with experimental data has been done. Moreover Comparison of base wind turbine with optimized one has been carried out.

3. Results and Discussion

The base airfoil which is applied for optimization process is E387 Eppler. The blade length is equal to 16.24m. The tip speed ratio (TSR) is 7 which mean Angular velocity is 6.17 rad/s. The wind speed is considered 15m/s. The angle of attack varies from -2.5 to 20.04 degrees and average Reynolds number of the flow is 4500000.

In the numerical simulation, the results must be independent of grid and domain. Also, numerical procedure and resultsmust be validated by comparing them with experiment and published data. The grid structure that is used in CFD for 2D simulation is created by a structured mesh, because of its simplicity and applicability to the current problem. This structured grid which is applied in this research illustrated in Fig.7

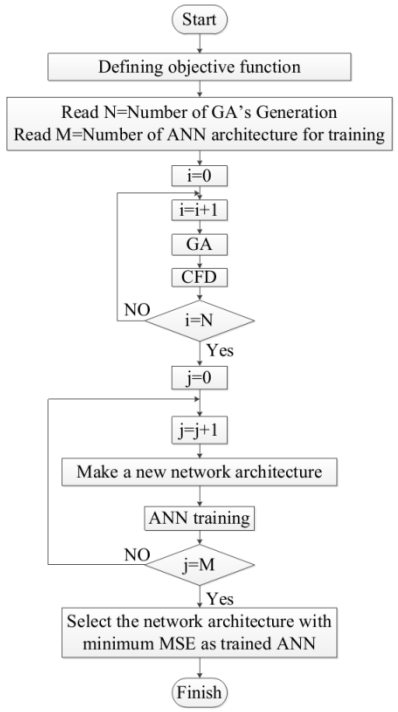

Fig.5. The flow chart utilized to train NN

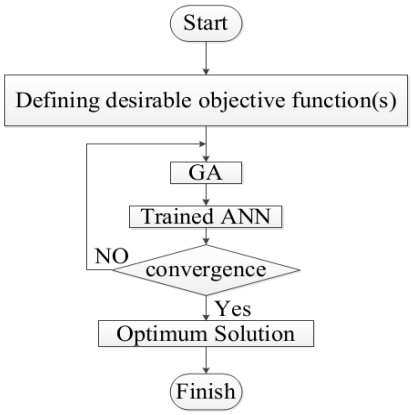

Fig.6. The flow chart to optimize with GA and NN

However the structure mesh has lower computational cost than unstructured mesh but, because of complexity of the wind turbine geometry, utilizing the unstructured mesh is necessary. The applied mesh in the domain is illustrated in Fig.8 and its detail view of the rotor is demonstrated in Fig.9. In addition, the rotor's configuration can be seen in Fig.10 .

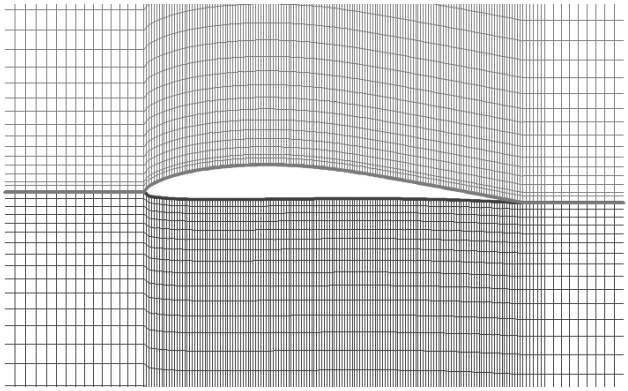

Fig.7. The part of the H Grid

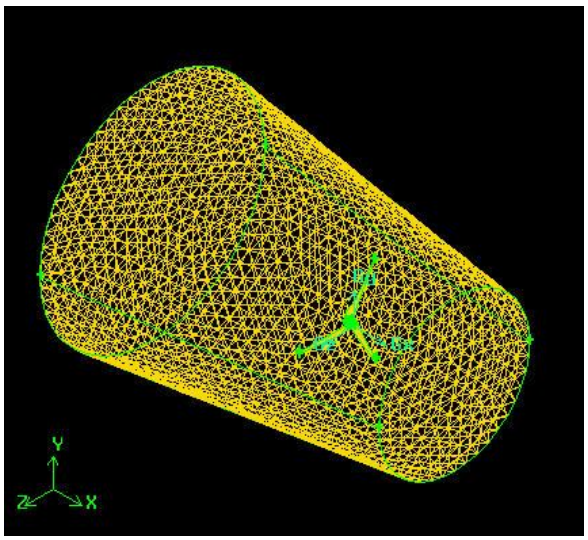

Fig.8. The mesh of the Domain

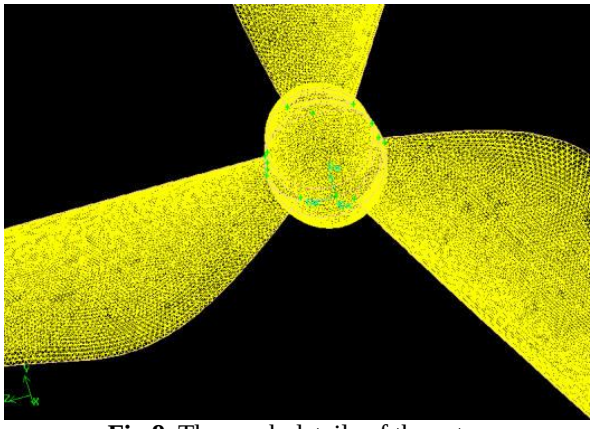

Fig.9. The mesh details of the rotor

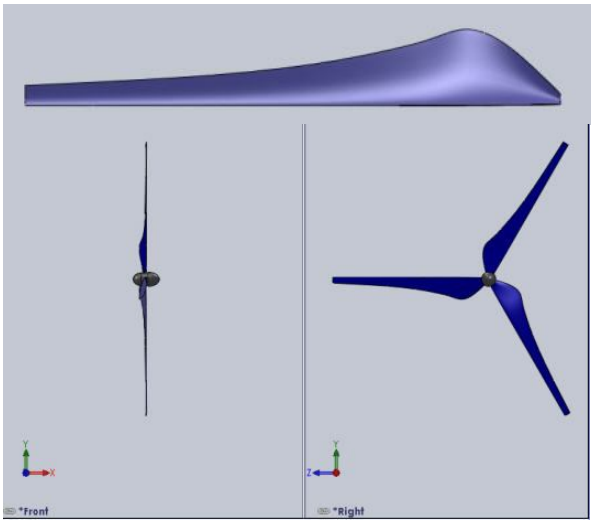

Fig.10. The rotor configuration of designed wind turbine

The domain and grid sizing is determined by doing several different trials. For instance, the effect of grid size is demonstrated inFig.11. According to this figure, to simulate the flow a mesh with 26650 numbers of nodes is utilized. In Fig.12, the pressure distribution on the surface of NACA0012 with zero angle of attack at Reynolds number equal to 6×10^6 is indicated and validated with experimental data [25]. These comparisons prove that the numerical results are in a good agreement with experimental data.

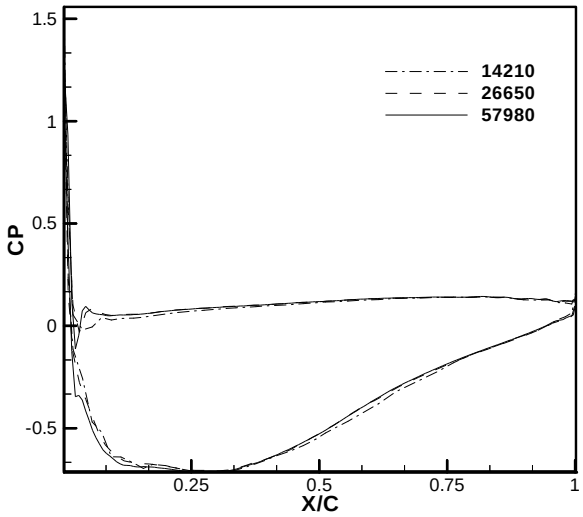

Fig.11. The effect of grid sizing on pressure distribution on the surface of the E387 airfoil for an angle of attack 1.6°

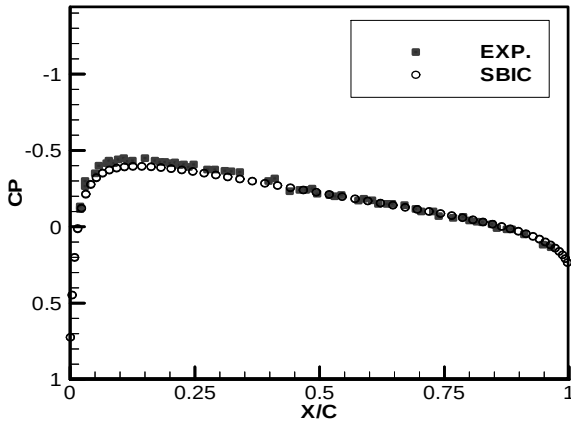

Fig.12. The comparison of numerical and experimental pressure coefficient distribution around airfoil NACA0012 with $\alpha = 0°$

Effects of domain length and grid size for 3D case have been examined. The influence of the domain length on moment coefficient(C_p) is presented in Fig.13. Moreover influence of grid sizing on C_p is manifests in Fig.14. These figures demonstrate the appropriate domain length and grid sizing.

The validation of 3D simulations has been carried out by comparing the numerical results with NREL phase VI wind turbine rotor. The pressure coefficient for 50% of the blade is illustrated in Fig.15.

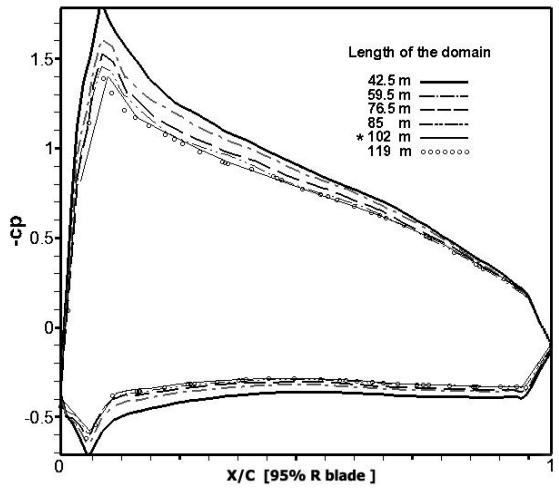

Fig.13. The influence of length on C_p

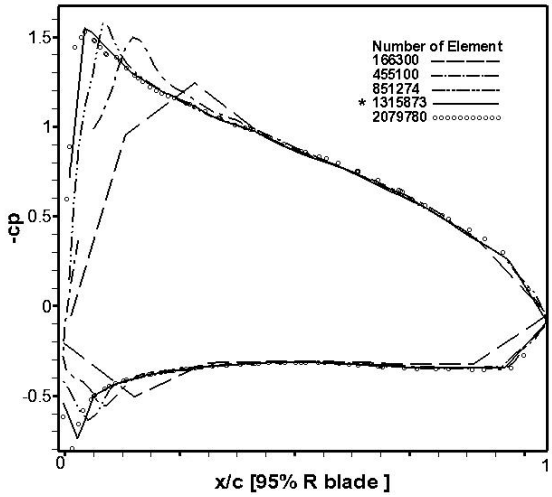

Fig.14. The influence of grid size on C_p

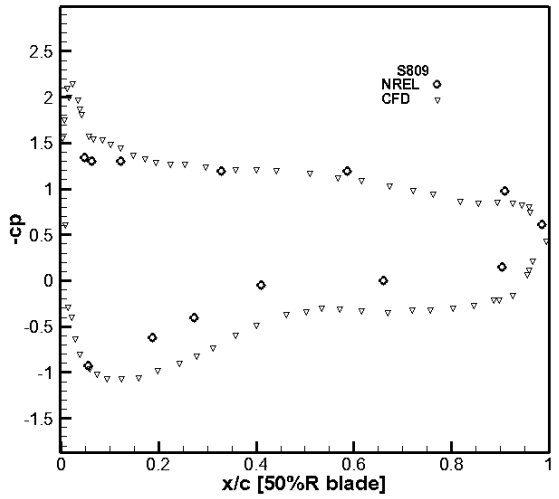

Fig.15. The pressure coefficient of the experiment data NREL phase VI and numerical result at 50% of the blade

The pressure coefficient distribution at 50% of the blade for present numerical simulation and experimental data is demonstrated in Fig.15. This comparison shows that there is a difference between these two results. This difference could be due to several parameters such, turbulent, separation phenomenon, wakes in downwind of the wind turbine, rotation of the blades and tip vorticesthat are not well predicted by the numerical simulation.

As mentioned before, MSE is selected as NN's performance. In other words, MSE is a measure to distinguish the ability of a network in predicting the targets.InFig.16, the performances of several examined networks architecture are illustrated. Horizontal axis of this figure is the network architecture, for example 8-8-3 means 8 neurons in first layer, 8 neurons in second layer and 3 neurons in output layer. Here, 8-8-3 is the best, because not only it has the lowest MSE, but also manifests no significant over fitting or under fitting and performances values are approximately equal for training, test, and validation sets.

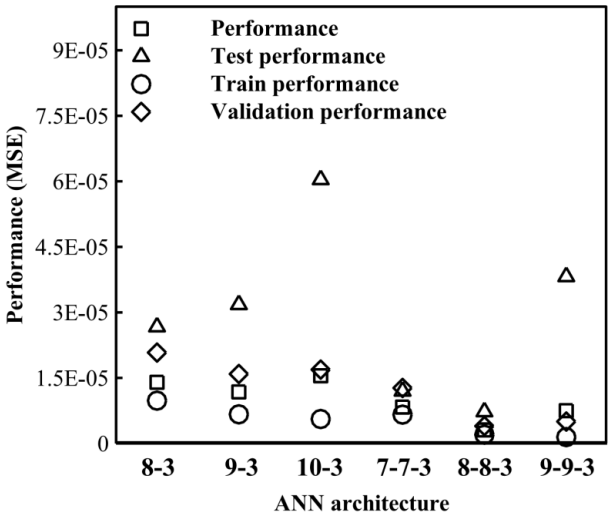

Fig.16. The performance of several networks architecture

The regression plot of this network's outputs with respect to targets is demonstrated inFig.17. It is important to note that in a perfect fitting, data must lie in 45 degree line i.e. the line whose outputs of the network is equal to the targets $(Output = Target)$.This figure indicates that suitable weight matrices are obtained and NN is able to predict the aerodynamic coefficients accurately. It can be concluded from these two figures that 8-8-3 Network is eligible to use as surrogate model therefore it is used for all optimizations which have been performed in this research.

Shape of optimized airfoils in respect to base airfoil at some angles of attack is illustrated in Fig.18. This figure shows that the airfoils at higher angles of attack are thicker because this postpones the separation. The comparison of pressure coefficient for both wind turbines, in spanwise direction are presented in Fig.19, Fig.20 and Fig.21.

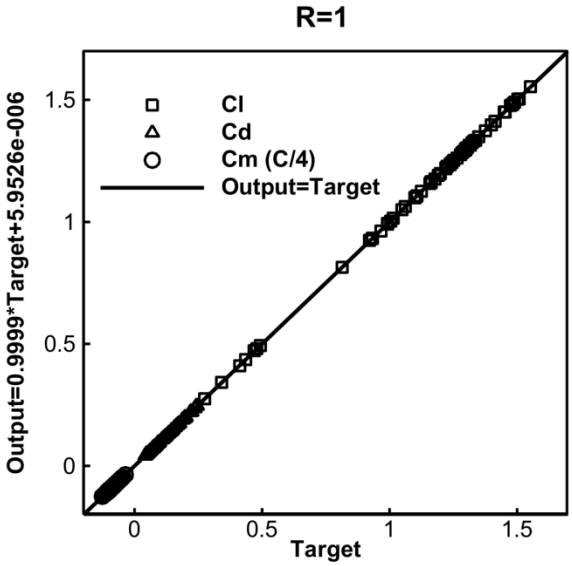

Fig.17. The regression plot of 8-8-3 network's outputs with respect to targets.

The area inside the pressure distribution diagram is equal to lift. These figures clearly rely that optimized blades produce the higher lift.

Power factor with respect to Tip Speed Ratio is illustrated in Fig.22. This figure confirms considerable improvement in power factor.

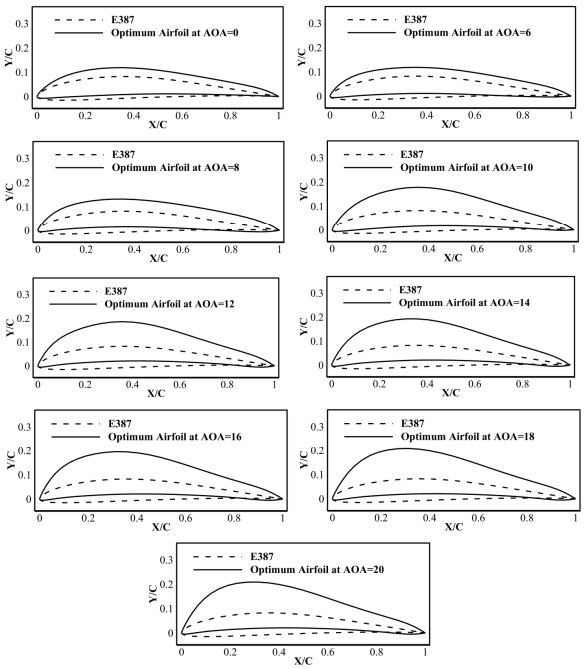

Fig.18. The shape of smart airfoil in respect to base airfoil at each AOA

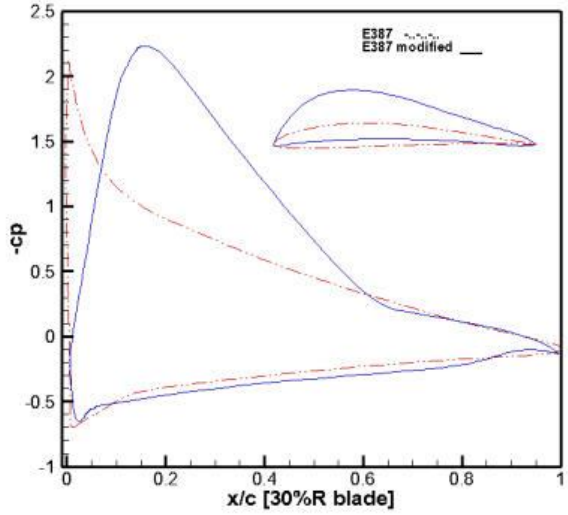

Fig.19. The pressure coefficient of base and optimized wind turbine in 30% of the blade

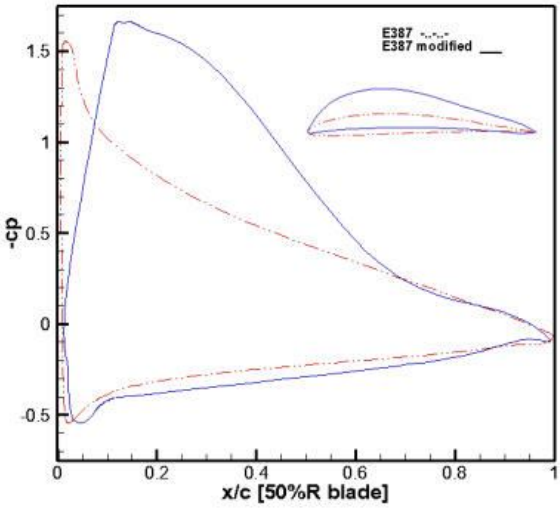

Fig.20. The pressure coefficient of base and optimized wind turbine in 50% of the blade

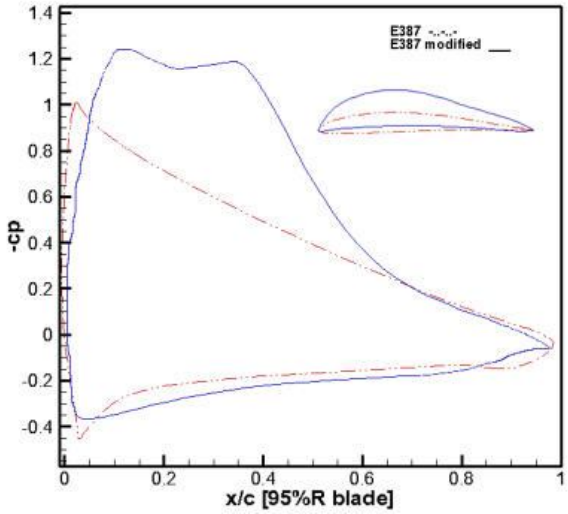

Fig.21. The pressure coefficient of base and optimized wind turbine in 95% of the blade

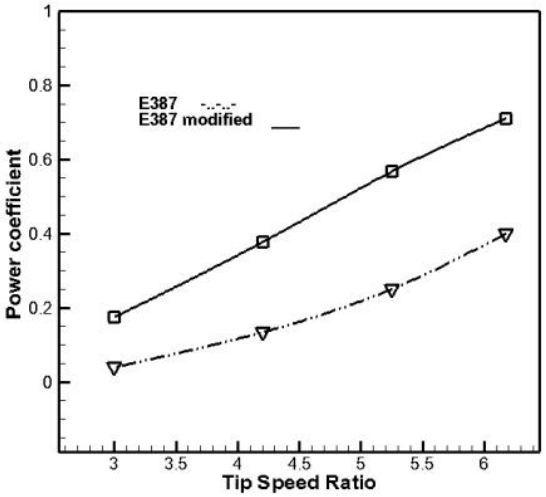

Fig.22. The power factor with respect to Tip Speed Ratio

4. CONCLUSION

In this article, a technique to high-fidelity aerodynamically optimization of a wind turbine blade presented which not only uses no simplifying assumption but also is very fast and practical. The main points can be summarized as follow.

1) The applied numerical method yield acceptable results of aerodynamic characteristics for both 2D and 3D cases.

2) The agreement between numerical result of trained NN and CFD simulation is considerable.

3) The results confirm that presented technique yield noticeable improvement in power factor.

4) The application of airfoils with high efficiency and good stall characteristics cause noticeable enhancement in wind turbine power factor.

5) The utilization of surrogate model in optimization process causes significant speed increase in optimization.

Nomenclature

GA	=	Genetic Algorithm
NVD	=	Normalized Variable Diagram
CFD	=	Computational Fluid Dynamic
k	=	Turbulence Model Parameter
ε	=	Turbulence Model Parameter
$\vec{S}$	=	Source Term
T	=	Time
CL	=	Lift Coefficient
CD	=	Drag Coefficient
c	=	Chord Length
AOA	=	Angle of Attack
ρ	=	Density
$\vec{V}$	=	Velocity Vector
$\vec{T}$	=	Stress Tensor
ϕ	=	Scalar Quantity
$\vec{q}$	=	Scalar Flux Vector
SBIC	=	Second and Blending Interpolation Combined
Γ	=	Diffusivity Coefficient
I^c	=	Convection Flux
I^D	=	Diffusion Flux
δv	=	Cell Volume
F	=	Mass Flux
A	=	Cell Face Area, convection-diffusion coefficient
$\overline{x}$	=	Normalized Coordinate
K	=	SBIC Parameter
P	=	Pressure
NN	=	Artificial Neural Network
μ	=	Dynamic Viscosity
N	=	Iteration Number
M	=	Iteration Number
dv	=	Displacement due to new Velocity
Re	=	Reynolds Number
SIMPLE	=	Semi-Implicit Method For Pressure – Linked Equation

References

[1] H. Sun, "Wind turbine airfoil design using response surface method", Journal of Mechanical Science and Technology, 25 , 1335-1340, 2011

[2] R.K. Singh, M.R. Ahmed, M.A. Zullah, Y.-H. Lee, "Design of a low Reynolds number airfoil for small horizontal axis wind turbines", Renewable Energy, 42, 66-76, 2012

[3] A.F.P. Ribeiro, A.M. Awruch, H.M. Gomes, "An airfoil optimization technique for wind turbines", Applied Mathematical Modelling, 36, 4898-4907, 2012

[4] M. Endo, Wind Turbine Airfoil Optimization by Particle Swarm Method. Case Western Reserve University, 2011.

[5] J.C.C. Henriques, F. Marques da Silva, A.I. Estanqueiro, L.M.C. Gato, "Design of a new urban wind turbine airfoil using a pressure-load inverse method", Renewable Energy, 34, 2728-2734, 2009

[6] J.C. Jouhaud, P. Sagaut, M. Montagnac, J. Laurenceau, "A surrogate-model based multidisciplinary shape optimization method with application to a 2D subsonic airfoil", Computers & Fluids, 36, 520-529, 2007

[7] C. Yan, H. Kyle, P. Russell, L. Yongsheng, B. Lihui, "Design Optimization of a Vertical Axis Wind Turbine Using a Genetic Algorithm and Surrogate Models", in: 12th AIAA Aviation Technology, Integration, and Operations (ATIO) Conference and 14th AIAA/ISSMO Multidisciplinary Analysis and Optimization Conference, American Institute of Aeronautics and Astronautics, 2012.

[8] S. Koziel, L. Leifsson, Airfoil Shape Optimization Using Variable-Fidelity Modeling and Shape-Preserving Response Prediction, in: X.-S. Yang, S. Koziel (Eds.) Computational Optimization and Applications in Engineering and Industry, Springer Berlin Heidelberg, pp. 99-124, 2011

[9] C. Thumthae, T. Chitsomboon, "Optimal angle of attack for untwisted blade wind turbine", Renewable Energy, 34, 1279-1284, 2009
[10] B. Biegel, M. Juelsgaard, M. Kraning, S. Boyd, J. Stoustrup, "Wind turbine pitch optimization, in: Control Applications (CCA)", IEEE International Conference on, pp. 1327-1334, 2011
[11] R.K. Singh, M.R. Ahmed, "Blade design and performance testing of a small wind turbine rotor for low wind speed applications", Renewable Energy, 50, 812-819, 2013
[12] M. Jureczko, M. Pawlak, A. Mężyk, "Optimisation of wind turbine blades", Journal of Materials Processing Technology, 167 463-471, 2005
[13] X. Liu, L. Wang, X. Tang, "Optimized linearization of chord and twist angle profiles for fixed-pitch fixed-speed wind turbine blades", Renewable Energy, 57, 111-119, 2013
[14] A. Sharifi, M.R.H. Nobari, "Prediction of optimum section pitch angle distribution along wind turbine blades", Energy Conversion and Management, 67, 342-350, 2013
[15] M.O.L. Hansen, Aerodynamics of wind turbines [electronic resource], Earthscan, 2008.
[16] B. Bavanish, K. Thyagarajan, "Optimization of power coefficient on a horizontal axis wind turbine using bem theory", Renewable and Sustainable Energy Reviews, 26 , 169-182, 2013
[17] J.R.P. Vaz, J.T. Pinho, A.L.A. Mesquita, "An extension of BEM method applied to horizontal-axis wind turbine design", Renewable Energy, 36, 1734-1740, 2011
[18] J.C. Dai, Y.P. Hu, D.S. Liu, X. Long, "Aerodynamic loads calculation and analysis for large scale wind turbine based on combining BEM modified theory with dynamic stall model", Renewable Energy, 36 1095-1104, 2011
[19] M. Djavareshkian, "A new NVD scheme in pressure-based finite-volume methods", 14th Aurtalasian Fluid Mechanics Conference, Adelaide University, Adelaide, Ausrtalia, pp. 339-342, 10-14 December ,2001
[20] B.P. Leonard, "A survey of finite differences with upwinding for numerical modeling of the incompressible convection diffusion equation" in C. Taylor and K. Morgan leds Technices in Transient and Turbulent Flow, Pineridgequess, Swansea, U.K., 2, 1-35, 1981
[21] R.M. Hicks, P.A. Henne, "Wing Design by Numerical Optimization", Journal of Aircraft, 15 407-412, 1978
[22] R.L. Haupt, S.E. Haupt, Practical Genetic Algorithms, A John Wiley & Sons, Inc., Publication, 2004.
[23] M.T. Hagan, H.B. Demuth, M. Beale, Neural network design, PWS Publishing Co., 1996.
[24] Y. Hao, M.W. Bogdan, Levenberg?Marquardt Training, in: Intelligent Systems, CRC Press, 2011, pp. 1-16.
[25] Experimental data base for computer program assessment, in, tech.rep.,AGARD.